

# Modeling Spectralon's bidirectional reflectance for in-flight calibration of Earth-orbiting sensors

Stéphane F. Flassac, Michel M. Verstraete  
*Institute for Remote Sensing Applications*  
*CEC Joint Research Centre, I-21020 Ispra (VA), Italy*

Bernard Pinty  
*Laboratoire de Météorologie Physique*  
*URA 2671 CNRS University Blaise Pascal, F-63177 Aubière, France*

Carol J. Bruegge  
*Jet Propulsion laboratory, California Institute of Technology*  
*4800 Oak Grove Drive, Pasadena, Ca. 91109, U.S.A.*

## ABSTRACT

The in-flight calibration of the EOS Multi-angle imaging SpectroRadiometer (MISR) will be achieved, in part, by observing deployable Spectralon panels. This material reflects light diffusely, and allows all cameras to view a near constant radiance field. This is particularly true when a panel is illuminated near the surface normal. To meet the challenging MISR calibration requirements, however, very accurate knowledge of the panel reflectance must be known for all utilized angles of illumination, and for all camera and monitoring photodiode view angles. It is believed that model predictions of the panels bidirectional reflectance distribution function (BRDF) can be used in conjunction with a measurements program to provide the required characterization. This paper describes the results of a model inversion which was conducted using measured Spectralon BRDF data at several illumination angles. Four physical parameters of the material were retrieved, and are available for use with the model to predict reflectance for any arbitrary illumination or view angle. With the test data the root mean square difference between the model and the observations is currently of the order of the noise in the data, at about  $\pm 1\%$ . With this success it is hoped that the model will be useful in a variety of future studies, including the development of a measurements test plan, the validation of these data, and the prediction of a new BRDF profile, should the material degrade in space.

## 1. INTRODUCTION

The in-flight calibration of the Multi-angle Imaging SpectroRadiometer (MISR) cameras will be achieved, in part, by observing deployable Spectralon panels. This material was selected because it is highly Lambertian (as compared to most other materials), spatially uniform, and has an established history of use in laboratory and field operations. As the calibration of MISR is to be accomplished to 3% in absolute accuracy and 0.5% in relative within band accuracy, the energy reflected from the panel must be known to a high degree of accuracy. The bidirectional reflectance distribution function (BRDF) will be characterized pre-flight, and monitored in-orbit using a set of photodiodes. These include nadir-viewing diodes, a diode mounted to a goniometer arm which swings in the nadir/ spacecraft-velocity plane, and two diodes which observe the panel at the same angle as the most-oblique viewing MISR cameras. Some sources of uncertainty will nevertheless remain with respect to the radiance collected by each of the cameras. For example, there is no guarantee that the pre-flight measured BRDF profile will be maintained, nor that the in-orbit measurements made by the diodes will exactly assess the energy reflected into the cameras. The diodes have a wide field-of-view, as compared to an individual MISR pixel within a camera, and do not view the cross-track range of view angles observed by the cameras. For these reasons it is believed that the merger of actual measurements with model predictions of performance can lead to the highest accuracy calibration. The use of independent approaches reduces systematic biases, and the model can be used to complement the diode data set collected in flight, should the panel degrade with time. Further, in this pre-launch era the model allows us to assess BRDF measurement sampling strategies. It is for these reasons that the research described in this paper was initiated. The success of the model at predicting reflecting characteristics of Spectralon has further application to the land-science community. It allows the reflecting properties to be better understood, for example, on comparable bright, highly diffusive surfaces, such as the calibration sites used by the remote sensing community.

This paper describes a first look at the suitability of various models to describe the bidirectional reflectance distribution function of Spectralon. This includes a discussion of the data sets, models, inversion procedures and preliminary results.

## 2. BIDIRECTIONAL REFLECTANCE DATA SETS

We have used a data set provided by Dr. Jim Irons (NASA/GSFC). The measurements were made under contract by TMA Technologies. Three lasers (at wavelengths 488, 632.8 and 1060 nm) were used to measure the BRDF of Spectralon. These light sources were intrinsically coherent and polarized. Although no polarization filters were placed in front of the sensor, two sets of measurements were taken, one for each of the polarizations of the incident beam (P-parallel and S-perpendicular to the plane of incidence). A total of 4 data sets were collected at illumination zenith angles of 2°, 20°, 40°, and 60° at each of the three wavelengths. All measurements were taken in the principal plane with the zenith angle varying from -89° to +89°. We have transformed the BRDF [sr<sup>-1</sup>] into the more commonly used BRF [dimensionless], by multiplying all values by  $\pi$ . From a purely physical point of view, this transformation was not absolutely necessary, but the models often work with reflectance factors.

Since the reflectance of a medium depends on the polarization of the incoming light, we analyzed the two polarizations separately. Significant non-random noise can be observed, especially at large viewing zenith angles, which may be related to the nature of the source of light (lasers produce speckles) or to inaccuracies in the angular positioning of the source or the sensor.

## 3. METHODOLOGY

A number of physically based and empirical models were tested with respect to their capability of describing the anisotropy of the Spectralon. These models use a limited number of parameters, whose values are retrieved by inverting the model against the data. This is achieved with the help of numerical optimization procedures. A global optimization technique<sup>3</sup>, coupling the exploring capabilities of Genetic Algorithms with the exploiting performance of a Quasi-Newton algorithm, was used to invert the models against the data.

The inversion minimizes the function  $\delta^2$ :

$$\delta^2 = \sum^N [BRF_{modeled} - BRF_{measured}]^2 \quad (1)$$

where N is the number of measurements.

The RMS of the fit between the model and the data is defined as follows:

$$RMS = \left( \frac{\delta^2}{N - P} \right)^{1/2} \quad (2)$$

where P is the number of model parameters to retrieve.

Model inversions were performed separately for each polarization and wavelength. Furthermore, since the MISR camera will not be observing the reference panels at angles larger than 68°, we have initially limited our modeling effort to the range [-80°, +80°].

## 4. MODELS AND RESULTS

### 4.1 MVBPI with P-polarization data set

MVBPI is a bidirectional reflectance model proposed by Pinty and Verstraete<sup>4</sup>. They developed a modeled bidirectional reflectance  $\rho$  of a semi-infinite, turbid medium illuminated from a direction  $(0, \phi_1)$  and observed from a direction  $(\theta_2, \phi_2)$ :

$$\rho = \rho(\omega, \Theta, \chi_p, r_A; \theta_1, \theta_2, \phi_1, \phi_2) \quad (3)$$

where  $\theta_1$  and  $\phi_1$  are the zenith and azimuth angles of illumination.  $\theta_2$  and  $\phi_2$  the zenith and azimuth angles of the observer,  $\omega$  is the average single scattering albedo of the particles making up the medium,  $\Theta$  is the asymmetry factor in the parameterized phase

function of Henyey-Greenstein,  $\chi_1$  is the parameter representing the average angle of the scattering element facets (used in the Goudriaan parameterization), and  $r\Lambda$  represents the structure of the medium. This parameter allows an explicit analytical description of the "hot spot", or opposition effect.

The results of the inversion of MVBP1 against the TMA measurements are presented in Table 1 and in Figure 1. The following points are worth noting:

- $\chi_1$  is very close to zero at all wavelengths. This implies that the Spectralon behaves as a turbid medium made up of scatterers with no preferential orientation.
- $\Theta$  is positive, indicating that light is propagated forward into the medium.
- $r\Lambda$  varies quite a lot between wavelengths and gives rather large values.

Figure 2 shows the relative contributions of single and multiple scattering to the total reflectance of the Spectralon. Clearly, an improvement of the analytical description of the reflectance will most likely be achieved in the multiple scattering contribution, which contributes 80% or more of the signal.

#### 4.2 MVBP6 with P-polarization data set

Most bidirectional reflectance models consider non-isotropic scatterers for the single scattering contribution only. Multiple scattering, which is difficult to treat analytically, is generally parameterized assuming isotropic scatterers. To improve on the description of the reflectance of the Spectralon, we have introduced a new parameterization of the multiple scattering contribution which accounts for the scatterers' anisotropy. This new model (MVBP6) will be described elsewhere.

The results of the inversion using MVBP6 against the F'-polarized data set are presented in Table 1 and Figure 3.

It can be seen that:

- The general fit is slightly better (by about 0.2% in RMS).
- The values of the structural parameter  $r\Lambda$  are much more stable, a desirable property since it should be independent of wavelength.
- $\chi_1$  remains very close to zero.

#### 4.3 Tests with S-polarization data set

Table 2 presents the results of the inversion of the same models against the S-polarized data set.

It can be seen that:

- The models cannot describe the reflectance of an S-polarized beam as well as a P-polarized, but the RMS remains at about 2%.
- In the S-polarization case, the improvement of MVBP6 over MVBP1 is not very significant, possibly due to the somewhat larger noise in the data set.

#### 4.4 Other tests and results

Table 3 exhibits the results of additional tests performed with other models and parameterizations:

- The results labeled MVBP5 were obtained by applying the model MVBP1 where the single scattering albedo  $\omega$  was modified according to the similarity relations of van de Hulst and Grossman<sup>6</sup>, as suggested by Pinty and Verstraete<sup>7</sup>. It appears that this solution performs as well as the unmodified MVBP1.
- The results labeled MVBP24 arc relative to the MVBP1 mode.1, where the Henyey-Greenstein phase function has been replaced by a Legendre polynomial representation of order 4. The RMS of the fit between this upgraded model and the data is as good as the one obtained with the MVBP6 model, but the parameter  $rA$  showed as much variability as was found with the MVBP1 model
- For reference, a polynomial of order 4 of the following form has been tested:

$$P = (c_1 + c_2\theta_1 + c_3\theta_1 + c_4\theta_1 + c_5\theta_1)(d_1 + d_2\theta_2 + d_3\theta_2 + d_4\theta_2 + d_5\theta_2) \quad (4)$$

It can be seen by inspection of Table 3 that an empirical formula of high degree is not capable of representing the bidirectional reflectance of the Spectralon as well as a physically-based model.

- Finally, MVBP1 and MVBP6 were inverted against reflectance data sets including view zenith angles up to 85°, Table 3 shows a slight degradation in the RMS of the fit, probably due to the higher noise level in the data at these large angles,

## 5. CONCLUSIONS

We can describe the bidirectional reflectance of the Spectralon and in particular its slight anisotropy with a physically-based model. The root mean square difference between the model and the observations is currently of the order of the noise in the data ( $\pm 1\%$ ). New investigations are currently on the way to improve the data base and to develop the model to attain even better results. It is expected that meaningful corrections to account for the anisotropy of the Spectralon panels will be achieved in the next few years and will improve the calibration of the MISR instrument.

## 6. ACKNOWLEDGEMENTS

The work of the first author is supported by a grant of the CEC-JRC, the first two authors acknowledge the financial support of the Exploratory Research Program of the JRC. The work of the fourth author is carried out by the Jet Propulsion Laboratory, California Institute of Technology, under contract with the National Aeronautics and Space Administration.

## 7. REFERENCES

1. C.J. Bruegge, V.G. Duval, N.J. Chrien, and D.J. Diner, "Calibration plans for the Multi-angle imaging SpectroRadiometer (MISR)," *Metrologia*, Submitted, 1993.
2. C.J. Bruegge, A.E. Stiegman, R.A. Rainen, and A.W. Springsteen, "Use of Spectralon as a diffuse reflectance standard for in-flight calibration of Earth-orbiting sensors," *Optical Engineering*, April, 1993.
3. J.M. Renders, S.P. Flasse, M.M. Verstraete, and J.P. Nordvik. "A comparative study of optimization methods for the retrieval of quantitative information from satellite data," Commission of the European Communities, Joint Research Centre JRC IILJR-14851 EN, Ispra, Italy, 1992.
4. M.M. Verstraete, B. Pinty, and R.E. Dickinson, "Bidirectional reflectance of vegetation canopies. Part I: Theory," *Journal of Geophysical Research*, 95: 11,755-11,765, 1990.
5. R. Pinty, M.M. Verstraete, and R.E. Dickinson, "Bidirectional reflectance of vegetation canopies. Part II: Inversion and validation," *Journal of Geophysical Research*, 95: 11,767-11,775, 1990.
6. H.C. van de Hulst and K. Grossman, "The atmospheres of Venus and Mars," in *The Atmospheres of Venus and Mars.*, Gordon and Breach, 1968.

7. B. Pinty and M.M. Verstraete, "On the design and validation of bidirectional reflectance and albedo models," *Remote Sensing Environment*, 41:155-167, 1992.

Table 1. Values of retrieved parameters for polarization-P, angles up to 80°

Model	$\lambda$	$\omega$	$\Theta$	$\chi_1$	$r\Lambda$	$a$	$b$	RMS
MVBP1	488.0	0.99966	0.21238	-0.02306	4.06766			0.01365
	632.8	0.99947	0.26725	-0.02750	2.17775			0.01282
	1060.0	0.99885	0.30842	-0.00055	1.23154			0.01532
MVBP6	488.0	0.99441	0.35323	0.00685	0.27064	1.34720	-0.10850	0.01139
	632.8	0.99582	0.37949	-0.00136	0.20552	1.34730	-0.33886	0.01144
	1060.0	0.99534	0.39236	-0.02435	0.19660	1.33498	-0.42807	0.01398

Table 2. Values of retrieved parameters for polarization-S, angles up to 80°

Model	$\lambda$	$\omega$	$e$	$\chi_1$	$r\Lambda$	$a$	$b$	RMS
MVBP1	488.0	0.99997	0.31151	-0.00650	147.12880			0.01466
	632.8	0.99937	0.31854	-0.02298	17.06090			0.02049
	1060.0	0.99893	0.35541	-0.03875	17.43342			0.02653
MVBP6	488.0	0.99999	0.30871	-0.00590	2.94.10075	1.06512	-0.75309	0.01467
	632.8	1.00000	0.30007	-0.02193	33.26712	1.51185	-1.95207	0.01994
	1060.0	1.00000	0.33705	-0.03459	28.95774	1.19859	-0.85723	0.02521

Table 3. RMS values of additional experiments

Model	$N_b$ parameter	$\lambda$	P-polarization Up to 80°	P-polarization Up to 85°	S-polarization up to 80°	S-polarization up to 85°
MVBP1	4	488.0	0.01365	0.01851	0.01466	0.01943
		632.8	0.01282	0.01587	0.02049	0.02767
		1060.0	0.01532	0.02069	0.02653	0.03257
MVBP6	6	488.0	0.01139	0.01275	0.01467	0.01932
		632.8	0.01144	0.01258	0.01994	0.02165
		1060.0	0.01398	0.01706	0.02520	0.03226
MVBP5	4	488.0	0.01365			
		632.8	0.01282			
		1060.0	0.01532			
MVBP24	7	488.0	0.01174			
		632.8	0.01091			
		1060.0	0.01414			
Polynomial	10	488.0	0.07691			
		632.8	0.08245			
		1060.0	0.08390			

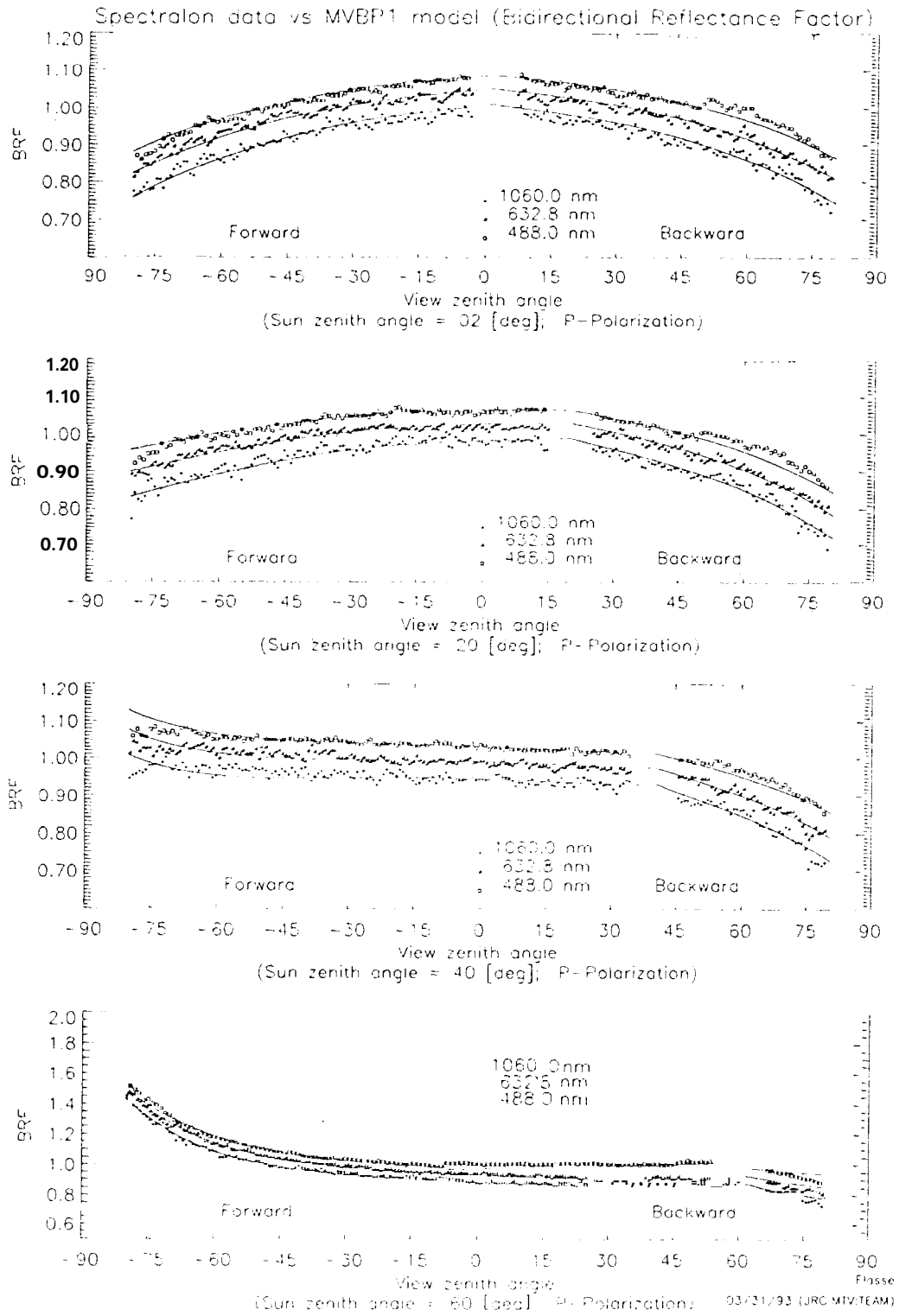


Figure 1. Observed (dots) and modeled using MVBP1 (solid line) bidirectional reflectance factors of a Spectralon panel as a junction of the view zenith angle, in the principal plane. Each frame exhibits the results for three wavelengths, at the indicated illumination zenith angle.

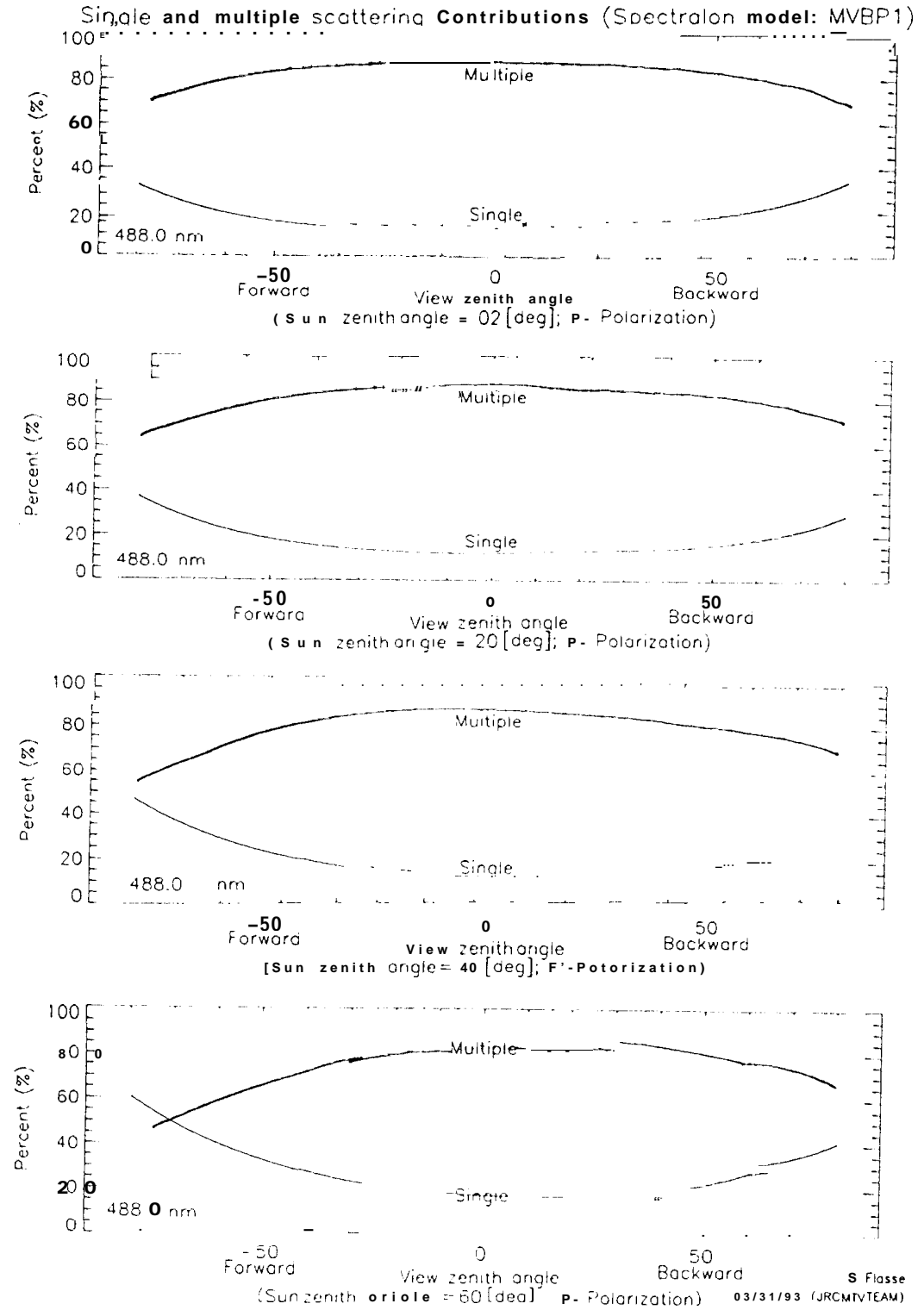


Figure 2. Single and multiple scattering contributions to the total reflectance of a Spectralon panel, as estimated by the model MVBP 1. The four frames correspond to the indicated illumination zenith angles.

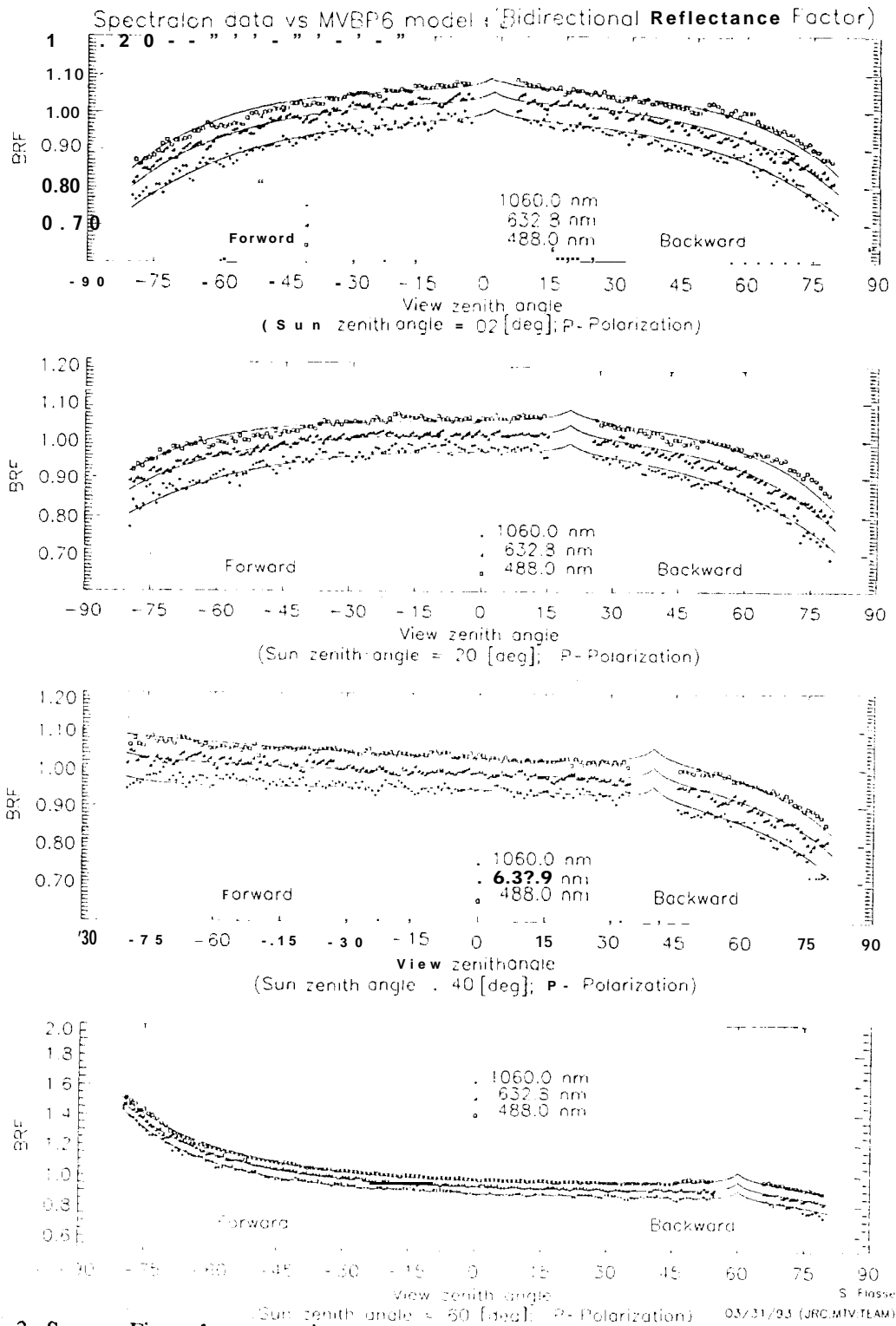


Figure 3. Same as Figure 1, except using model MVBP6.